

## Analysis of $\gamma$ - $\gamma$ Cascades by Polarization and Directional Correlation: Decay of $\text{Rh}^{101}_{\sigma\ddagger}$

G. T. WOOD\*

*University of Pennsylvania, Philadelphia, Pennsylvania*

and

*Argonne National Laboratory, Argonne, Illinois*

AND

S. KOIČKI† AND A. KOIČKI‡

*University of Pennsylvania, Philadelphia, Pennsylvania*

(Received 20 April 1966)

A procedure is given for using the results of polarization-direction correlation and directional-correlation measurements to analyze  $\gamma$ - $\gamma$  cascades in cases in which both transitions may be of mixed multipole order. A method is also presented for obtaining polarization-direction correlation coefficients from the measured rates via a Monte Carlo program based on Compton-scattering theory. The methods were applied to the 198-127-keV  $\gamma$ - $\gamma$  cascade in  $\text{Ru}^{101}$  populated by the decay of  $\text{Rh}^{101}_{\sigma}$ . It was determined that the spin of the 127-keV state is  $\frac{3}{2}$  and the spin of the 325-keV state is  $\frac{1}{2}^+$ . The  $E2/M1$  mixing ratio is  $0.17 \pm 0.04$  for the 127-keV transition and  $-0.12 \pm 0.03$  for the 198-keV one. Relative  $\gamma$ -ray intensities of 94, 100, and 21, respectively, were found for the 127-, 198-, and 325-keV transitions. In a triple-coincidence scintillation-counter measurement, the  $K$  internal-conversion coefficient of the 127-keV transition was found to be  $0.16 \pm 0.02$ .

### I. INTRODUCTION

FROM a measurement of the directional correlation of a  $\gamma$ - $\gamma$  cascade following radioactive nuclear decay, it is often possible to determine the angular momenta of the levels populated by the cascade. However, if one or both of the  $\gamma$  rays is possibly a mixed-multipole transition, the analysis of directional-correlation data may not lead to a unique determination of the angular momenta. Such cases require additional data. Several authors<sup>1-4</sup> have discussed the use of polarization-correlation data for this purpose in cases in which there is only one mixing ratio to determine. The doubly mixed  $\gamma$ - $\gamma$  cascades in which both  $\gamma$  rays are mixed multipoles are particularly difficult to analyze since two unquantized parameters must be fitted precisely. Here directional-correlation measurements may be fitted by a continuous set of the two mixing ratios. If, however, the directional-correlation data are combined with polarization-direction correlation data, it is then possible by appropriate analysis to obtain a unique interpretation or at worst a small number of possible interpretations. In the cases in which the interpretation is not unique, it may be easy to choose between the different possibilities with the aid of other data.

When only one mixing ratio in a  $\gamma$ - $\gamma$  cascade is un-

determined, polarization-correlation measurements may be used to select from among the possible assignments that fit the directional-correlation data. In this role, relatively crude polarization-correlation data may be good enough to make possible the selection, since the precise value of the mixing ratio is determined from the directional-correlation measurement. However, in the present case in which both  $\gamma$  rays are mixed, the accuracy of the determination of the mixing ratios will depend directly on the accuracy of the polarization-correlation measurements. To gain this accuracy, the effects should be large. Thus in the case of double mixtures, polarization correlation is best applied to low-energy  $\gamma$  rays (say 100-500 keV) where the sensitivity of the Compton polarimeter to polarization is high. Fortunately, from this point of view, the doubly mixed  $\gamma$ - $\gamma$  cascades prevalent in the odd- $A$  and odd-odd nuclei are also frequently low in energy.

Although the Compton polarimeter is most sensitive at low energies, it will yield accurate results only when "calibrated" properly; i.e., one must accurately determine the transformation between the measured rates and the polarization-direction correlation coefficients. It is sometimes possible to determine this transformation by measuring  $\gamma$  rays of known polarization. However, in such a determination it is not always possible or convenient to reproduce the energy and geometrical conditions of the actual experiment and, moreover, the empirical method of calibration is subject to the usual errors of measurement. Clearly, a theoretical method of obtaining the polarization sensitivity would be both convenient and useful. For the case of point detectors, the polarization sensitivity of the Compton polarimeter may easily be calculated from the theoretical Klein-Nishina formula. In practice, however, one is forced to

† Work supported by the National Science Foundation and the U. S. Atomic Energy Commission.

\* Present address: Argonne National Laboratory, Argonne, Illinois.

‡ Present address: Boris Kidric Institute, Belgrade, Yugoslavia.  
<sup>1</sup> G. T. Wood, Ph.D. thesis, Washington University, 1956 (unpublished); P. S. Jastram, G. T. Wood, and J. P. Hurley, *Bull. Am. Phys. Soc.* **3**, 65 (1958).

<sup>2</sup> C. F. Coleman, *Nucl. Phys.* **5**, 495 (1958).

<sup>3</sup> G. T. Wood, *Phys. Rev.* **116**, 1499 (1959).

<sup>4</sup> G. T. Wood, *Nucl. Phys.* **32**, 411 (1962).

use detector dimensions that are far from ideal in order to realize reasonable counting rates and one must, therefore, perform an average over the finite size of the detectors. Since the  $\gamma$  ray may scatter more than once in the scatterer crystal, it is reasonable to employ the Monte Carlo method to do this averaging. We have written a Monte Carlo program for this purpose and some of the steps involved are summarized in Sec. IV and in the Appendix.

In this paper we apply the angular-correlation method to the 3-yr  $K$ -capture decay of  $\text{Rh}^{101\sigma}$  to  $\text{Ru}^{101}$ . Previous investigations of this decay include measurements of  $\gamma$ -ray spectra,<sup>5-10</sup> directional correlation,<sup>7,8,10,11</sup> and electron internal-conversion spectra.<sup>7,8,12,13</sup> Also, the  $\gamma$ -ray angular distribution following the Coulomb excitation of  $\text{Ru}^{101}$  has been measured.<sup>14,15</sup> In addition to the angular-correlation measurements, we have also measured  $\gamma$ -ray intensities and the internal-conversion coefficient  $\alpha_K$  of the 127-keV ground-state transition.

## II. THEORY OF ANGULAR-CORRELATION ANALYSIS

The theory of angular correlation has been given by Biedenharn and Rose.<sup>16</sup> Ferentz and Rosenzweig,<sup>17</sup> using a somewhat different notation, have calculated  $F$  coefficients. Let  $j_1$ ,  $j$ , and  $j_2$  be the initial, intermediate, and final spins, respectively, of the  $\gamma$ - $\gamma$  cascade. The first transition  $\gamma_1$  is a mixture of  $2^{L_1}$  and  $2^{L_1+1}$  poles with a mixing ratio  $\delta_1$ , and the second transition  $\gamma_2$  is a mixture of  $2^{L_2}$  and  $2^{L_2+1}$  poles with a mixing ratio  $\delta_2$ .

The  $\gamma$ - $\gamma$  direction-correlation function is

$$W(\theta) = 1 + \sum_{\nu} A_{\nu} P_{\nu}(\cos\theta), \quad (1)$$

where  $\nu = 2, 4, \dots, \nu_{\max}$  ( $\frac{1}{2}\nu_{\max}$  being the smallest of the quantities  $j$ ,  $L_1+1$ , and  $L_2+1$ ),  $\theta$  is the angle between the gamma rays, and

$$A_{\nu} = a_{\nu}^{(1)} a_{\nu}^{(2)},$$

<sup>5</sup> N. N. Perrin, Ann. Phys. (N.Y.) 5, 71 (1960).

<sup>6</sup> R. A. Ricci, S. Monaro, G. B. Vingiani, D. R. Speranza, and R. van Lieshout, Nuovo Cimento Suppl. 19, 339 (1961).

<sup>7</sup> J. S. Evans and R. A. Naumann, Phys. Rev. 140, B559 (1965).

<sup>8</sup> P. I. Connors and A. Schwarzschild (private communication); P. I. Connors, Ph.D. thesis, Pennsylvania State University, 1966 (unpublished).

<sup>9</sup> N. K. Aras, G. D. O'Kelley, and G. Chilosi, Phys. Rev. 146, 869 (1966).

<sup>10</sup> G. Chilosi, K. E. G. Löbner, R. Moro, P. R. Speranza, and G. B. Vingiani (to be published).

<sup>11</sup> N. Goldberg, Bull. Am. Phys. Soc. 2, 230 (1957).

<sup>12</sup> L. Marquez, Phys. Rev. 95, 67 (1954).

<sup>13</sup> K. Hisatake, S. Matsuo, and H. Kawakami, J. Phys. Soc. Japan 20, 1107 (1965).

<sup>14</sup> R. C. Ritter, P. H. Stelson, F. K. McGowan, and R. L. Robinson, Phys. Rev. 128, 2320 (1962).

<sup>15</sup> G. M. Temmer and N. P. Heydenberg, Phys. Rev. 104, 967 (1956).

<sup>16</sup> L. C. Biedenharn and M. E. Rose, Rev. Mod. Phys. 25, 729 (1953).

<sup>17</sup> M. Ferentz and N. Rosenzweig, Argonne National Laboratory Report No. ANL-5324, 1955 (unpublished).

$$a_{\nu}^{(1)} = [F_{\nu}(L_1 L_1 j_1 j) + 2\delta_1 F_{\nu}(L_1 L_1 + 1 j_1 j) + \delta_1^2 F_{\nu}(L_1 + 1 L_1 + 1 j_1 j)] / (1 + \delta_1^2),$$

$$a_{\nu}^{(2)} = [F_{\nu}(L_2 L_2 j_2 j) + 2\delta_2 F_{\nu}(L_2 L_2 + 1 j_2 j) + \delta_2^2 F_{\nu}(L_2 + 1 L_2 + 1 j_2 j)] / (1 + \delta_2^2).$$

If the angle  $\phi^{(1)}$  between the plane of polarization of  $\gamma_1$  and the normal to the plane of  $\gamma_1$  and  $\gamma_2$  is also measured, then we have a measurement of the polarization-direction correlation given by the probability function

$$\omega(\theta, \phi^{(1)}) = 1 + \sum_{\nu} A_{\nu} P_{\nu}(\cos\theta) + [\sum_{\nu} B_{\nu}^{(1)} P_{\nu}^2(\cos\theta)] \cos 2\phi^{(1)}, \quad (2)$$

where

$$B_{\nu}^{(1)} = b_{\nu}^{(1)} a_{\nu}^{(2)},$$

$$b_{\nu}^{(1)} = (-1)^{\sigma(L_1+1)} [-D_{\nu}(L_1 L_1) F_{\nu}(L_1 L_1 j_1 j) + 2\delta_1 D_{\nu}(L_1 L_1 + 1) F_{\nu}(L_1 L_1 + 1 j_1 j) + \delta_1^2 D_{\nu}(L_1 + 1 L_1 + 1) F_{\nu}(L_1 + 1 L_1 + 1 j_1 j)] / (1 + \delta_1^2),$$

$$D_{\nu}(LL) = \frac{(\nu-2)!}{(\nu+2)!} \frac{2\nu(\nu+1)L(L+1)}{\nu(\nu+1)-2L(L+1)},$$

$$D_{\nu}(LL+1) = \frac{(\nu-2)!}{(\nu+2)!} 2(L+1),$$

and where  $\sigma(L_1+1)$  is 0 if the  $L_1+1$  pole is electric and 1 if this pole is magnetic.

If, instead, the polarization of  $\gamma_2$  is measured, we have

$$\omega(\theta, \phi^{(2)}) = 1 + \sum_{\nu} A_{\nu} P_{\nu}(\cos\theta) + [\sum_{\nu} B_{\nu}^{(2)} P_{\nu}^2(\cos\theta)] \cos 2\phi^{(2)}, \quad (3)$$

where

$$B_{\nu}^{(2)} = a_{\nu}^{(1)} b_{\nu}^{(2)},$$

$$b_{\nu}^{(2)} = (-1)^{\sigma(L_2+1)} [-D_{\nu}(L_2 L_2) F_{\nu}(L_2 L_2 j_2 j) + 2\delta_2 D_{\nu}(L_2 L_2 + 1) F_{\nu}(L_2 L_2 + 1 j_2 j) + \delta_2^2 D_{\nu}(L_2 + 1 L_2 + 1) F_{\nu}(L_2 + 1 L_2 + 1 j_2 j)] / (1 + \delta_2^2).$$

In order to determine the coefficients  $A_{\nu}$  and  $B_{\nu}^{(i)}$  (in which  $i=1$  or  $2$  designates the transition whose polarization is measured), it is necessary to measure  $W(\theta)$  and the two distributions  $W(\theta, \phi^{(i)})$ . From Eqs. (2) and (3) it is clear that measurements need only be made at two of the angles  $\phi^{(i)}$ , i.e.,  $\phi = 0^\circ$  and  $90^\circ$ . If  $\nu_{\max} = 4$ , it is sufficient to measure the  $W(\theta, \phi^{(i)})$  at only two values of  $\theta$ , for example, at  $\theta = 90^\circ$  and  $135^\circ$ . However, if the transition  $i$  is known to be a dipole-quadrupole mixture, it is necessary to measure  $W(\theta, \phi^{(i)})$  at only one angle  $\theta$  (say  $\theta = 90^\circ$  since the polarization effect is usually maximum at this angle). In this case the coefficient  $B_4^{(i)} = D_4(22)A_4 = A_4/12$  and is, therefore, actually determined from the directional-correlation measurement. Consequently, in this case of a dipole-quadrupole

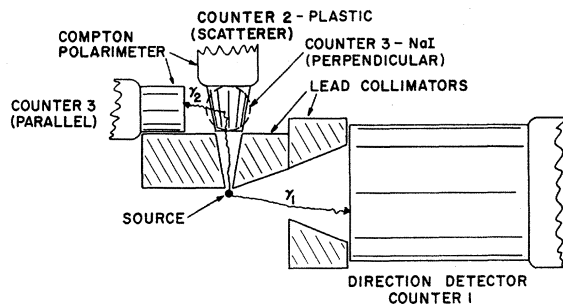


FIG. 1. The arrangement of scintillation detectors for  $\gamma$ - $\gamma$  polarization-direction-correlation measurements. Counter 1:  $4\frac{1}{2}$ -in.-diameter  $\times$  6-in.-long NaI(Tl) on Amperex 58 AVP photomultiplier. Counter 2: Truncated cone of NE 102 plastic scintillator,  $1\frac{1}{2}$  in. in diameter at the base  $\times$   $1\frac{1}{2}$  in. long, on RCA 7746 photomultiplier. Counter 3:  $1\frac{1}{2}$ -in.-diameter  $\times$   $1\frac{1}{2}$ -in.-long NaI(Tl), integral mount.

mixture, a measurement of  $W(\theta, \phi^{(i)})$  at two values of  $\theta$  yields no more information than at one angle.

To determine the spin and mixing assignment, it is helpful to define

$$M_{\nu}^{(i)} \equiv B_{\nu}^{(i)} / A_{\nu} = b_{\nu}^{(i)} / a_{\nu}^{(i)}. \quad (4)$$

We note that the  $M_{\nu}^{(1)}$  depend only on  $j_1$ ,  $j$ , and  $\delta_1$  of  $\gamma_1$  while the  $M_{\nu}^{(2)}$  depend only on  $j$ ,  $j_2$ , and  $\delta_2$  of  $\gamma_2$ . Thus for each possible pair of spins  $j_1$ ,  $j$  we may deduce two possible mixing ratios  $\delta_1$  and  $\delta_1'$  from a measurement of  $M_2^{(1)}$ . Likewise, a measurement of  $M_2^{(2)}$  will do the same for  $\gamma_2$ . For each spin and parity sequence  $j_1(\pi_1)$ ,  $j(\pi)$ ,  $j_2(\pi_2)$  that we consider, there will therefore be four mixing-ratio assignments  $\delta_1$ ,  $\delta_1'$ ,  $\delta_2$ , and  $\delta_2'$  consistent with  $M_2^{(1)}$  and  $M_2^{(2)}$ . For each of these possible assignments we may calculate  $A_2$  and  $A_4$  and rule out those possibilities that do not agree with the measured values of  $A_2$  and  $A_4$ . In this way a unique assignment or a small number of possible assignments will be found consistent with the combined directional- and polarization-correlation data.

### III. POLARIZATION-CORRELATION APPARATUS

The polarization-correlation apparatus was similar to a system discussed previously by one of the authors.<sup>3</sup> It consists of three scintillation counters arranged as shown in Fig. 1. The direction of one gamma ray  $\gamma_d$  in the cascade is determined by the "direction detector"—counter 1, a NaI(Tl) crystal  $4\frac{1}{2}$  in. in diameter and 6 in. long and collimated with lead. Both the polarization and the direction of the other gamma ray  $\gamma_p$  are determined by the "polarization detector," a two-crystal Compton polarimeter consisting of counters 2 and 3. The scattering occurs in a truncated cone of plastic scintillator (counter 2, which has a base diameter of  $1\frac{1}{2}$  in. and a height of  $1\frac{1}{2}$  in.) and the scattered  $\gamma_p$  is detected in the  $1\frac{1}{2}$ -in.-diam.  $\times$   $1\frac{1}{2}$ -in.-long NaI(Tl) crystal (counter 3). A lead collimator shields counter 3 from direct radiation. The degree of polarization of the  $\gamma$

rays entering the polarization detector is measured for a given angle  $\Theta$  between counters 1 and 2 by measuring the relative rates of scattering of these  $\gamma$  rays into counter 3 for the two orientations of counter 3 (parallel and perpendicular to the plane defined by the axes of counters 1 and 2).

The electronics consisted of a conventional transistorized fast-slow coincidence system. The pulses from counters 2 and 3 were summed electronically by a pulse-adding circuit. The full-energy peak in the sum spectrum was selected by a pulse-height selector. A second pulse-height selector placed a relatively wide window on the pulses from counter 2 alone in order to limit the range of scattering angles of  $\gamma_p$  in the scatterer and also to reduce  $\gamma$ -ray scattering from counter 3 into counter 2. Coincidences between the two pulse-height selector pulses were detected by a slow coincidence circuit (resolving time  $\tau \approx 10^{-6}$  sec) which yielded the "polarimeter pulses." Coincidences were also detected between counters 1 and 2 with tunnel-diode fast-coincidence circuitry (resolving time  $\tau \approx 10^{-8}$  sec). The fast-coincidence pulses, the polarimeter pulses, and the pulses from a third pulse-height selector set on the photopeak of  $\gamma_d$  in counter 1 were combined in slow coincidence to give the fast-slow coincidence pulses between the direction counter and the polarimeter. At each of the two positions of counter 3, the coincidence rate was normalized by the polarimeter rate, determined concurrently. The two normalized rates are denoted  $N_X$  and  $N_Y$ , where  $X$  refers to the parallel orientation and  $Y$  to the perpendicular orientation of counter 3.

### IV. DETERMINATION OF THE POLARIZATION-DIRECTION CORRELATION COEFFICIENTS

Starting with Eq. (2), Appendix I shows that

$$S(\Theta) \equiv \frac{N_X - N_Y}{N_X + N_Y} = \sum_{\nu=2}^{\nu_{\max}} F_{\nu}(\Theta) B_{\nu}. \quad (5)$$

In addition to  $\Theta$ , the factors  $F_{\nu}(\Theta)$  depend on the angles of scattering of the detected  $\gamma$  rays, the finite size of the

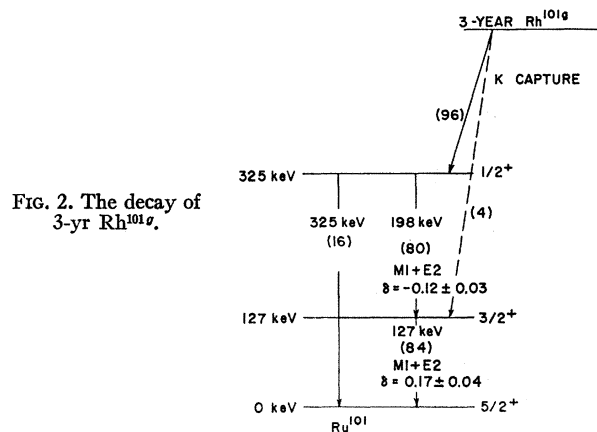


FIG. 2. The decay of 3-yr  $\text{Rh}^{101}$ .

detectors, the pulse-height selection in counter 2, and the incident  $\gamma$ -ray energy. This factor, which is defined by Eq. (8) in Appendix I, may be calculated from the theory of Compton scattering by a Monte Carlo calculation as discussed in Appendix II. A Monte Carlo FORTRAN program which computes  $F_2(\pi/2)$  has been written<sup>18</sup> for the Argonne CDC-3600 digital computer. An experimental test of the Monte Carlo computation is given in Appendix III.

As discussed in Sec. II,  $B_4 = A_4/12$  when  $\gamma_p$  is a dipole-quadrupole mixture. For this case, therefore, it follows that  $B_4 = 0$  if  $A_4 = 0$  and  $B_2$  may be determined from measurements of  $S(\Theta)$  at a single angle  $\Theta = \pi/2$ , since Eq. (5) then yields

$$B_2 = S(\pi/2)/F_2(\pi/2), \quad (6)$$

where  $F_2(\pi/2)$  is obtained from the Monte Carlo computation.

### V. GAMMA-RAY SPECTRA AND INTERNAL-CONVERSION MEASUREMENTS

Three-yr  $\text{Rh}^{101g}$  decays<sup>13</sup> by  $K$  capture to  $\text{Ru}^{101}$  are shown in Fig. 2. The  $\gamma$ -ray spectrum (Fig. 3) of this decay was measured with a thin-window NaI(Tl) scintillation counter measuring  $1\frac{1}{2}$  in. in diameter  $\times$  1 in. long. The radioactive source used in this measurement and in all of our studies was produced by cyclotron irradiation<sup>11</sup> in 1957 so that the shorter lived components 4.5-day  $\text{Rh}^{101m}$  and 206-day  $\text{Rh}^{102}$  have largely decayed out. However, the small component of the spectrum above the 325-keV photopeak is attributed to the decay<sup>13</sup> of 2.1-yr  $\text{Rh}^{102m}$ . From Fig. 3 we have obtained the  $\gamma$ -ray intensity ratios  $I_{127}/I_{198} = 0.94$  and  $I_{325}/I_{198} = 0.21$ . The photopeak efficiencies required to obtain these intensities were computed by a Monte Carlo calculation.<sup>19</sup>

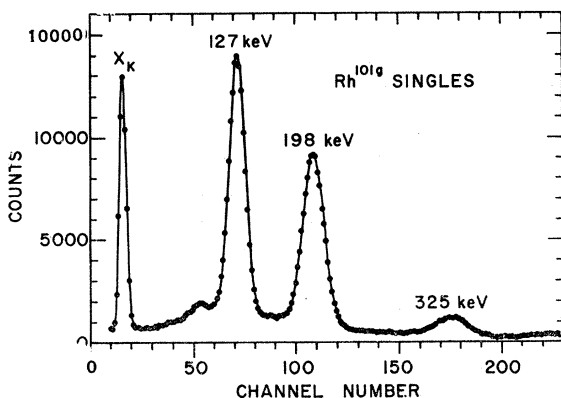


FIG. 3. The  $\gamma$ -ray singles spectrum of  $\text{Rh}^{101g}$  in a thin-window NaI(Tl) crystal measuring  $1\frac{1}{2}$  in. in diameter  $\times$  1 in. long.

<sup>18</sup> G. T. Wood, Argonne National Laboratory Physics Division Informal Report PHY-1965 C (unpublished). This report, which includes the FORTRAN listing, is available from the author.

<sup>19</sup> W. F. Miller and W. J. Snow, Argonne National Laboratory Report No. ANL-6318 (unpublished).

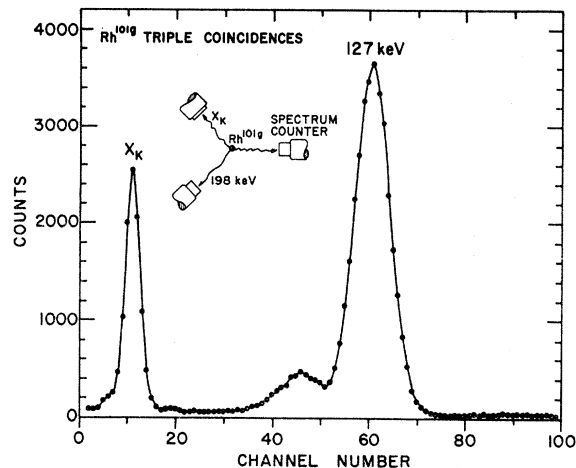


FIG. 4. The spectrum of  $\gamma$  rays in triple coincidence with  $K$ -shell  $x$  rays and 198-keV  $\gamma$  rays.

From the singles spectrum in Fig. 3, one might attempt to obtain the internal-conversion coefficients of the 127- and 198-keV  $\gamma$  rays and the  $x$ -ray peak. However, this analysis would be complicated by the presence of electron-capture  $x$  rays which are indistinguishable from the  $K$ -shell  $x$  rays associated with internal conversion of the two  $\gamma$  rays. Moreover, the  $K$ -capture branching ratio to the first and second excited states is not precisely known even though the  $\gamma$ -ray intensities show that the  $K$  capture goes mostly to the 352-keV state. In order to overcome these difficulties, we have performed a triple-coincidence measurement with a crystal arrangement shown in Fig. 4. In this arrangement we observe the spectrum in counter 1 [thin window, NaI(Tl) crystal,  $1\frac{1}{2}$  in. in diameter, 1 in. long] in coincidence with  $K$ -shell  $x$  rays in a thin NaI(Tl) crystal (counter 2) and 198-keV  $\gamma$  rays in a 2-in.-diameter  $\times$  2-in.-long NaI(Tl) crystal (counter 3). For this configuration it may be shown that the number of  $x$  rays detected in counter 2 in triple coincidence is just twice the number of  $K$ -shell  $x$  rays associated with the internal conversion of the 127-keV transition. Thus the  $K$  conversion of the 127-keV transition is given by half the ratio of the  $K$ -shell  $x$ -ray intensity to the 127-keV  $\gamma$ -ray intensity. After taking into account suitable corrections for photopeak efficiencies,  $x$ -ray escape in the case of the 127-keV photopeak, the fluorescent yield of Ru, and the directional correlation between the 127- and 198-keV  $\gamma$  rays, we obtain  $\alpha_K^{127} = 0.16 \pm 0.02$ .

Knowing  $\alpha_K$  for the 127-keV transition, our  $\gamma$ -ray intensity ratio  $I_{\gamma_{127}}/I_{\gamma_{198}} = 0.94$ , and the intensity ratio of  $K$  internal-conversion electrons  $I_{e_{198}}/I_{e_{127}} = 0.274$  deduced from Hisatake's<sup>13</sup> relative-intensity measurements (the data collected 1580 days after bombardment), we determine  $\alpha_K^{198} = 0.041$ . The total transition intensities given in Fig. 2 are based on our  $\gamma$ -ray intensity ratios and the  $\alpha_K$  given above.

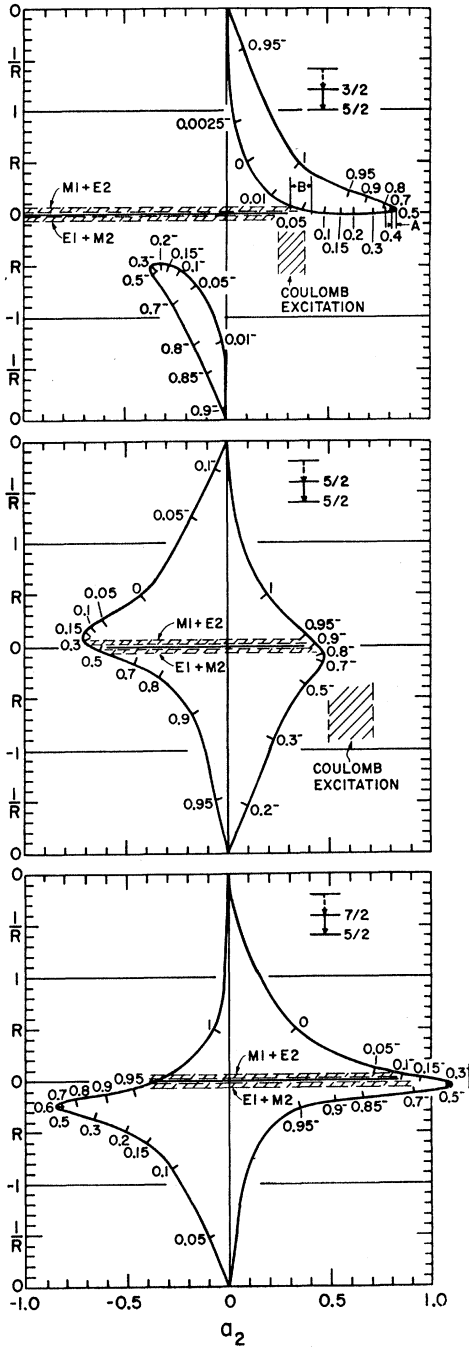


FIG. 5. The analysis of the 127-keV transition. The solid curves give  $R$  versus  $a_2$  for transitions with spin sequence  $\frac{7}{2}^+ \rightarrow \frac{5}{2}^+$ ,  $\frac{5}{2}^+ \rightarrow \frac{5}{2}^+$ , and  $\frac{3}{2}^+ \rightarrow \frac{5}{2}^+$ , where  $R = b_2/a_2$  for  $E1+M2$  transitions and  $-b_2/a_2$  for  $M1+E2$  transitions. These curves are parametric in the quadrupole content  $\delta^2/(1+\delta^2)$ , where  $\delta$  is the quadrupole/dipole mixing ratio. The quantity  $R$  can vary from 0 to  $\pm\infty$ . Therefore, when  $|R| > 1$ ,  $1/R$  is plotted instead of  $R$  so that the whole range may be conveniently presented. The limits that  $\gamma\text{-}\gamma$  angular correlation measurements set upon  $R$  are indicated by the horizontal dashed lines for the two choices of transition character. The limits specified by the vertical dashed lines are derived from angular-distribution measurements of  $\gamma$  rays following Coulomb excitation.

TABLE I. Results of polarization-direction correlation measurements.

Measurement	$S(\pi/2)$	$F_2(\pi/2)$	$B_2$
Pol 127-Dir 198	$-0.015 \pm 0.007$	$1.764 \pm 0.015$	$-0.008 \pm 0.004$
Pol 198-Dir 127	$-0.094 \pm 0.007$	$1.751 \pm 0.015$	$-0.053 \pm 0.004$

## VI. ANGULAR-CORRELATION RESULTS

The angular-correlation results include both directional-correlation and polarization-direction-correlation measurements on the 198–127-keV  $\gamma\text{-}\gamma$  cascade in Ru<sup>101</sup>.

Expressing the directional correlation as an expansion in Legendre polynomials  $W(\theta) = 1 + A_2 P_2(\cos\theta) + A_4 P_4(\cos\theta)$  and correcting for the finite size of detectors, we obtain  $A_2 = 0.195 \pm 0.008$  and  $A_4 = 0.008 \pm 0.012$ . These results are in agreement with Goldberg,<sup>11</sup> who obtained  $A_2 = 0.184 \pm 0.018$  and  $A_4 = 0.016 \pm 0.023$ , and with Chilosi and Löbner,<sup>10</sup> who obtained  $A_2 = 0.181 \pm 0.025$  and  $A_4 = 0.020 \pm 0.034$ .

Two polarization-direction correlation measurements were performed for the 127- and 198-keV gamma rays. We call these the “pol. 127-dir. 198” and the “pol. 198-dir. 127” correlations. The results of these measurements are given in Table I, where the experimental quantity  $S(\pi/2)$  is defined by Eq. (5) and the polarization-direction correlation coefficient  $B_2$  is obtained from Eq. (6), which applies since  $A_4$  is practically zero. The function  $F_2(\pi/2)$  was computed with the Monte Carlo program as discussed in Sec. IV.

## VII. INTERPRETATION OF THE ANGULAR-CORRELATION RESULTS

To begin the interpretation of the 198–127-keV  $\gamma\text{-}\gamma$  cascade, we assume that the ground-state spin<sup>20</sup> is  $\frac{5}{2}^+$ . Also, from the internal-conversion-coefficient data given in Sec. V, it is known that the 127- and 198-keV  $\gamma$  rays are both predominantly  $M1$  with some  $E2$  admixture. Therefore, the angular momentum  $J$  of the 127-keV state is limited to the values  $\frac{3}{2}^+$ ,  $\frac{5}{2}^+$ , and  $\frac{7}{2}^+$ , while the angular momentum  $J'$  of the 325-keV state must be  $(J-1)^+$ ,  $J^+$ , or  $(J+1)^+$ .

As discussed in Sec. VI, the angular-correlation experiments yielded three parameters, namely,  $A_2 = 0.195 \pm 0.008$ ,  $B_2^{(127)} = -0.008 \pm 0.004$ , and  $B_2^{(198)} = -0.053 \pm 0.004$ , in which the number in parentheses refers to the energy (in keV) of  $\gamma_p$ . The ratio  $b_2^{(127)}/a_2^{(127)}$  may be analyzed to decide between the three possible spin sequences  $\frac{7}{2}^+ \rightarrow \frac{5}{2}^+$ ,  $\frac{5}{2}^+ \rightarrow \frac{5}{2}^+$ , and  $\frac{3}{2}^+ \rightarrow \frac{5}{2}^+$  for the states involved in the 127-keV transition. This analysis is shown in Fig. 5, where  $R$ , which is  $-b_2/a_2$  for  $M1+E2$  mixtures and  $b_2/a_2$  for  $E1+M2$  mixtures, is drawn (solid curves) as a function of  $a_2$ . These curves are parametric in the quadrupole content  $\delta^2/(1+\delta^2)$ , where  $\delta$  is the quadrupole/dipole mixing ratio. The experimental limits on

<sup>20</sup> J. H. E. Griffiths and J. Owen, Proc. Phys. Soc. (London) **A65**, 951 (1952).

$R$  are specified by the horizontal crosshatched lines (upper set for mixtures of  $M1+E2$  and lower for mixtures of  $E1+M2$ ). Since the internal-conversion data indicate that the 127-keV transition is mostly  $M1$ , the possibility of an  $E1+M2$  mixture may be rejected. Furthermore, an  $E1+M2$  mixture is unlikely, since for all such possibilities an unreasonably large  $M2$  admixture would be required to fit the angular-correlation results. When only  $M1+E2$  mixtures are considered, Fig. 5 shows that for each of the three spins there are two  $E2/M1$  mixing ratios  $\delta$  that fit the  $b_2^{(127)}/a_2^{(127)}$  ratio.

There are nine possibilities of spin sequence to be analyzed for the 198-keV transition (three for each possible spin sequence of the 127-keV  $\gamma$  ray). Three of these are analyzed in Fig. 6 in a way similar to that in Fig. 5. Since  $R$  is a double-valued function of  $\delta$  for eight of the possibilities of spin sequence and single-valued in one (the  $\frac{3}{2} \rightarrow \frac{3}{2}$  case), 34 combinations (again rejecting  $E1+M2$  mixtures) of spin sequence and  $E2/M1$  mixing ratios for the 198-127-keV  $\gamma$ - $\gamma$  cascade are found to fit the two ratios  $b_2^{(127)}/a_2^{(127)}$  and  $b_2^{(198)}/a_2^{(198)}$  above. Of these 34, about 8 are reasonably consistent with the measured values of  $A_2$  and  $A_4$ . Consequently, the angular-correlation analysis does not turn out to be unique in this case. However, all but two of these possibilities (one with spin sequence  $\frac{1}{2} \rightarrow \frac{3}{2} \rightarrow \frac{5}{2}$  and the other  $\frac{3}{2} \rightarrow \frac{7}{2} \rightarrow \frac{5}{2}$ ) require that at least one of the two transitions have a large  $E2/M1$  mixing ratio (198-keV transition greater than  $\sim 98\%E2$  and 127-keV transition greater than  $\sim 30\%E2$ ) and so may be rejected on the basis of the internal-conversion data in Sec. V. Furthermore, angular-distribution measurements of the 127-keV  $\gamma$  ray following Coulomb excitation<sup>14,15</sup> are consistent with the  $\frac{1}{2} \rightarrow \frac{3}{2} \rightarrow \frac{5}{2}$  case and clearly rule out the  $\frac{3}{2} \rightarrow \frac{7}{2} \rightarrow \frac{5}{2}$  one. Thus, on the assumption that the  $\frac{1}{2} \rightarrow \frac{3}{2} \rightarrow \frac{5}{2}$  sequence is the correct one, the  $\gamma$ - $\gamma$  angular-correlation experiments yield an  $E2/M1$  mixing ratio of  $-0.12 \pm 0.03$  for the 198-keV transition and  $0.17 \pm 0.04$  for the 127-keV one.

The complexity of the foregoing analysis is considerably reduced if the Coulomb-excitation data are used immediately together with  $b_2^{(127)}/a_2^{(127)}$  as shown in Fig. 5, since then  $a_2^{(127)}$  may also be determined. The  $\gamma$ -ray directional-distribution coefficient of the 127-keV  $\gamma$  ray following Coulomb excitation has the form  $1 + A_2^{\text{Coul}} P_2(\cos\theta)$ , where  $A_2^{\text{Coul}} = 0.114 \pm 0.022$ .<sup>14</sup> The coefficient  $a_2^{(127)}$  may be obtained from  $a_2^{(127)} = A_2^{\text{Coul}} / F_2(22\frac{5}{2}j)$  and depends on  $J$ . Thus  $a_2^{(127)} = 0.317 \pm 0.06$  if  $J = \frac{3}{2}$ ,  $0.598 \pm 0.11$  if  $J = \frac{5}{2}$ , and  $-1.463 \pm 0.28$  if  $J = \frac{7}{2}$ . The limits imposed on  $a_2^{(127)}$  by the Coulomb-excitation data are indicated by the vertical dashed lines in Fig. 5; and with the horizontal limits set by  $b_2^{(127)}/a_2^{(127)}$ , the possibilities are confined to a single rectangular area for each spin case. Thus  $J = \frac{7}{2}$  is completely rejected. The case  $J = \frac{5}{2}$  is possible but requires a nearly pure  $E2$  127-keV transition, which is inconsistent with the internal-conversion measurement.

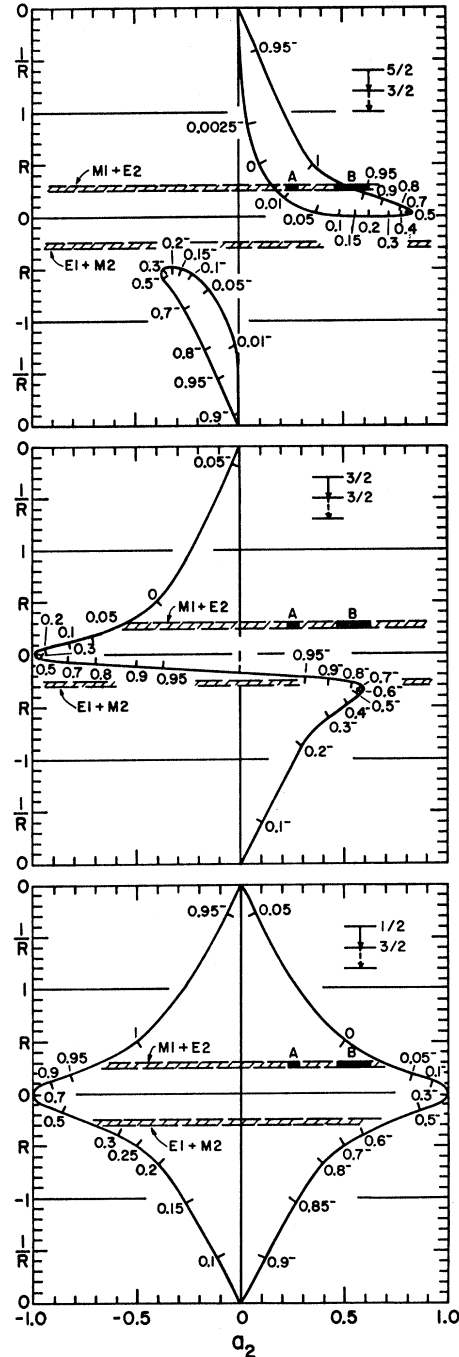


FIG. 6. Analysis of the 198-keV transition. The solid curves give  $R$  versus  $a_2$  for transitions with spin sequence  $\frac{1}{2} \rightarrow \frac{3}{2}$ ,  $\frac{3}{2} \rightarrow \frac{3}{2}$ , and  $\frac{3}{2} \rightarrow \frac{5}{2}$ . The limits on  $R$  determined by  $\gamma$ - $\gamma$  angular-correlation measurements are indicated by the horizontal dashed lines for the two choices of transition character. In the spin  $\frac{3}{2} \rightarrow \frac{5}{2}$  case of Fig. 5, the horizontal dashed lines determined  $a_2^{(127)}$  to lie in the  $A$  or  $B$  regions indicated. Since  $a_2^{(198)} = A_2/a_2^{(127)}$ , the quantity  $a_2^{(198)}$  is also restricted for  $J \rightarrow \frac{3}{2} \rightarrow \frac{5}{2}$  cascades, as indicated by the solid rectangles  $A$  and  $B$  in this figure.

Only the  $J = \frac{3}{2}$  case remains. Once the parameters of the 127-keV transition are established in this way, the 198-keV transition may be analyzed in a similar way.

The parameter  $a_2^{(198)} = A_2/a_2^{(127)}$  may be used together with  $b_2^{(198)}/a_2^{(198)}$  to restrict the possibilities to the rectangular regions  $B$  indicated on the three graphs in Fig. 6. The  $J' = \frac{3}{2}$  case is completely rejected. The case  $J' = \frac{5}{2}$  requires a nearly pure  $E2$  transition and is again inconsistent with the internal-conversion measurements. The spin  $J' = \frac{1}{2}$  case remains.

#### APPENDIX I: DERIVATION OF EQ. (5)

Equation (2) may be written in the form

$$\omega(\theta, \phi) = W(\theta) + W_p(\theta) \cos 2\phi,$$

where

$$W(\theta) = 1 + \sum_{\nu=2}^{\nu_{\max}} A_\nu P_\nu(\cos\theta),$$

and

$$W_p(\theta) = \sum_{\nu=2}^{\nu_{\max}} B_\nu P_\nu^2(\cos\theta).$$

Define  $\omega_{11}^i \equiv \omega(\theta^i, \pi/2)$  and  $\omega_{10}^i \equiv \omega(\theta^i, 0)$  for the  $i$ th triple coincidence. Then the probabilities of triple-coincidence detection for the two orientations of counter 3 are proportional to

$$n_X^i = \omega_{11}^i P_{11X}^i + \omega_{10}^i P_{10X}^i,$$

and

$$n_Y^i = \omega_{11}^i P_{11Y}^i + \omega_{10}^i P_{10Y}^i,$$

respectively, where (for example)  $P_{11X}^i$  represents the probability that a gamma ray  $\gamma_p$  initially polarized in the plane of angle  $\theta$  (i.e.,  $\phi = 90^\circ$  for event  $i$ ) will be scattered to the  $X$  (parallel) position of counter 3.

Let

$$\begin{aligned} \epsilon_X^i &\equiv P_{10X}^i - P_{11X}^i, & \epsilon_Y^i &\equiv P_{10Y}^i - P_{11Y}^i, \\ P_{11X}^i + P_{10X}^i &\equiv 1, & P_{11Y}^i + P_{10Y}^i &\equiv 1. \end{aligned}$$

Then it may be shown that

$$\begin{aligned} n_X^i &= \frac{1}{2} [W(\theta^i) + \epsilon_X^i W_p(\theta^i)], \\ n_Y^i &= \frac{1}{2} [W(\theta^i) - \epsilon_Y^i W_p(\theta^i)]. \end{aligned}$$

Now the measured triple-coincidence rates  $N_X$  and  $N_Y$  may be related to the probabilities  $n_X^i$  and  $n_Y^i$  through

$$\begin{aligned} N_X &\propto \langle n_X^i \rangle_X = \frac{1}{2} [\langle W(\theta^i) \rangle_X + \langle \epsilon_X^i W_p(\theta^i) \rangle_X], \\ N_Y &\propto \langle n_Y^i \rangle_Y = \frac{1}{2} [\langle W(\theta^i) \rangle_Y - \langle \epsilon_Y^i W_p(\theta^i) \rangle_Y], \end{aligned}$$

where  $\langle \rangle_X$  designates an average over  $X$  events and  $\langle \rangle_Y$  over  $Y$  events. Define

$$\begin{aligned} W(\Theta) &\equiv \frac{1}{2} [\langle W(\theta^i) \rangle_X + \langle W(\theta^i) \rangle_Y], \\ \Delta W(\Theta) &\equiv \frac{1}{2} [\langle W(\theta^i) \rangle_X - \langle W(\theta^i) \rangle_Y], \\ E(\Theta) &\equiv \frac{1}{2} [\langle \epsilon_X^i W_p(\theta^i) \rangle_X + \langle \epsilon_Y^i W_p(\theta^i) \rangle_Y], \\ \Delta E(\Theta) &\equiv \frac{1}{2} [\langle \epsilon_X^i W_p(\theta^i) \rangle_X - \langle \epsilon_Y^i W_p(\theta^i) \rangle_Y], \end{aligned}$$

where  $\Theta$  is the angle (measured at the source) between the two directional detectors (counters 1 and 2). In

terms of these quantities we may write

$$S(\Theta) \equiv \frac{N_X - N_Y}{N_X + N_Y} = \frac{E(\Theta) + \Delta W(\Theta)}{W(\Theta) + \Delta E(\Theta)}.$$

The terms  $\Delta W(\Theta)$  and  $\Delta E(\Theta)$  usually prove in practice to be negligible, so that  $S(\Theta) \approx E(\Theta)/W(\Theta)$ . Finally, this expression may be written in the form

$$\begin{aligned} S(\Theta) &\approx \sum_{\nu=2}^{\nu_{\max}} \epsilon_\nu B_\nu P_\nu^2(\cos\Theta) / (1 + \sum_{\nu=2}^{\nu_{\max}} G_\nu A_\nu P_\nu(\cos\Theta)) \\ &= \sum_{\nu=2}^{\nu_{\max}} F_\nu(\Theta) B_\nu, \end{aligned} \quad (7)$$

where

$$\begin{aligned} G_\nu &= \frac{\langle P_\nu(\cos\theta^i) \rangle_X + \langle P_\nu(\cos\theta^i) \rangle_Y}{2P_\nu(\cos\Theta)}, \\ \epsilon_\nu &= \frac{\langle \epsilon^i P_\nu^2(\cos\theta^i) \rangle_X + \langle \epsilon^i P_\nu^2(\cos\theta^i) \rangle_Y}{2P_\nu^2(\cos\Theta)}, \end{aligned} \quad (8)$$

$$F_\nu(\Theta) = \epsilon_\nu P_\nu^2(\cos\Theta) / W(\Theta).$$

The  $G_\nu$  are the directional-correlation attenuation factors (for counters 1 and 2) while the  $\epsilon_\nu$  are called the polarization-detector efficiencies. For an ideal configuration in which very small detectors are placed to detect  $90^\circ$  scattering of  $\gamma_p$  and for low  $\gamma$ -ray energies ( $\sim 100$  keV), the  $\epsilon_\nu$  will approach unity. For high  $\gamma$ -ray energies with large detectors placed close to the source, the  $\epsilon_\nu$  approach zero.

#### APPENDIX II: THEORY OF COMPTON SCATTERING AND THE MONTE CARLO METHOD

In order to calculate the polarization-detection efficiencies and the directional-correlation attenuation coefficients defined in Eq. (8), it is necessary to employ the theory of Compton scattering in a form suitable for application to multiple-scatter events as well as single scatters in the scatterer crystal. A theory convenient for this purpose has been given by Wightman,<sup>21</sup> who used a density-matrix formalism.

A photon entering the polarimeter is represented by the wave function  $\psi = C_1\psi_1 + C_2\psi_2$ , where  $\psi_1$  and  $\psi_2$  are two eigenstates representing the two independent states of linear polarization. The state of polarization of the beam of photons incident on the scatterer is represented by a diagonal  $2 \times 2$  density matrix  $\rho_{ij} = \langle C_i^* C_j \rangle_{av}$ , where the average is over the many photons in the beam. A photon beam fully polarized in the plane of the two cascade  $\gamma$  rays is represented by the density matrix  $\begin{pmatrix} 1 & 0 \\ 0 & 0 \end{pmatrix}$  and a beam polarized in the

<sup>21</sup> A. Wightman, Phys. Rev. 74, 1813 (1948).

corresponding perpendicular direction by the density matrix  $\begin{pmatrix} 0 & 0 \\ 0 & 1 \end{pmatrix}$ . With each scattering that occurs in the scatterer, the state of polarization is altered and consequently the density matrix undergoes transformation. The matrix  $\mathbf{S}$  that produces this transformation is given by Wightman<sup>21</sup> and depends on the linear-momentum vector of the photon before and after scattering. For single scattering, the final density matrix is then given by  $\rho_{\text{final}} = \rho_{\text{initial}} \mathbf{S}$ , where  $\rho_{\text{initial}}$  is the initial density matrix. If  $n$  scatters occur, then  $\rho_{\text{final}} = \rho_{\text{initial}} \mathbf{S}^1 \mathbf{S}^2 \cdots \mathbf{S}^n$ , where  $\mathbf{S}^j$  represents the transformation matrix for the  $j$ th scatter. After the first scatter, the density matrix ordinarily becomes nondiagonal. To interpret it physically, we must consider the response of the detector of scattered  $\gamma$  rays (counter 3) to the multiple-scattered  $\gamma$  ray. For this purpose we must also know the density matrix that characterizes the detector's sensitivity to linear polarization. In our case the detector (counter 3) is insensitive to polarization and its sensitivity is represented by the density matrix

$$\rho_{\text{det}} = \begin{pmatrix} \frac{1}{2} & 0 \\ 0 & \frac{1}{2} \end{pmatrix}.$$

Finally, the probability of detecting a given multiple-scattered photon is given by the trace ( $\rho_{\text{final}} \rho_{\text{det}}$ ). Thus for each event  $i$  we may calculate the quantities  $P_{11X}^i$  and  $P_{1X}^i$  needed to calculate  $\epsilon^i$  and  $F_{\nu}(\Theta)$ . The expressions are

$$P_{11X}^i = \text{Tr} \left[ \begin{pmatrix} 1 & 0 \\ 0 & 0 \end{pmatrix} \mathbf{S}^1 \mathbf{S}^2 \cdots \mathbf{S}^n \begin{pmatrix} \frac{1}{2} & 0 \\ 0 & \frac{1}{2} \end{pmatrix} \right],$$

$$P_{1X}^i = \text{Tr} \left[ \begin{pmatrix} 0 & 0 \\ 0 & 1 \end{pmatrix} \mathbf{S}^1 \mathbf{S}^2 \cdots \mathbf{S}^n \begin{pmatrix} \frac{1}{2} & 0 \\ 0 & \frac{1}{2} \end{pmatrix} \right],$$

where the  $\mathbf{S}^j$  in this case cause scattering to the position of counter 3 in its  $X$  orientation.

In applying the Monte Carlo method, it is desired to follow the photon as it undergoes scattering processes in the scatterer and is finally detected in the detector (counter 3). The mathematical techniques for doing this in the case in which polarization effects may be neglected are well known and have been used extensively. In the present case, in which polarization effects must be considered, it is possible as well as advantageous to first neglect polarization and make use of the published

method (we follow Cashwell and Everett<sup>22</sup>). In this approach, polarization effects need to be considered only for those Monte Carlo histories that result in detection. Thus, most of the events that do not result in detection are treated without the complications of polarization. For those histories  $i$  resulting in detection, the efficiencies  $\epsilon_X^i = P_{1X}^i - P_{11X}^i$  and  $\epsilon_Y^i = P_{11Y}^i - P_{1Y}^i$  are computed as discussed in Appendix I. Finally, the polarization-detection efficiencies  $\epsilon_{\nu}$  and the factors  $F_{\nu}(\Theta)$  must be calculated by averaging according to Eq. (8) over all histories resulting in detection. In averaging, proper weight is given to the various histories in proportion to the product of  $W(\theta^i)$  and the probability that the photon makes a first scatter. The first weight factor is necessary since the  $\gamma$ - $\gamma$  coincidence is forced, while the second weight factor is necessary since the first scatter of  $\gamma_p$  is forced.<sup>22</sup>

### APPENDIX III: EXPERIMENTAL TEST OF MONTE CARLO PROGRAM

In order to test the Monte Carlo program, polarization-direction correlation and directional-correlation measurements were performed on the 1409-keV-122-keV  $\gamma$ - $\gamma$  cascade in  $\text{Sm}^{152}$  populated in the  $K$ -capture decay of 13-yr  $\text{Eu}^{152}$  with the apparatus shown in Fig. 1. The  $\text{Eu}^{152}$  source was in a solid form and consequently the directional correlation ( $A_2 = 0.163 \pm 0.002$ ) was significantly attenuated relative to the value that would have been obtained if a liquid source were used. However, since  $\gamma_p$  (the 122-keV gamma ray) is known to be pure  $E2$ , the polarization-direction correlation coefficient  $B_2$  in this case is directly related to the measured directional-correlation coefficient  $A_2$  by the expression  $B_2 = -\frac{1}{2}A_2$ . The polarization-direction-correlation experiment yielded a value  $S(\pi/2) = -0.142 \pm 0.006$ . Consequently, we may determine  $F_2(\pi/2)$  experimentally from the calculation

$$F_2(\pi/2) = S(\pi/2)/B_2 = -2S(\pi/2)/A_2 \\ = 1.74 \pm 0.08.$$

The Monte Carlo calculation yields

$$F_2(\pi/2) = 1.733 \pm 0.017,$$

which agrees well with the experimental result. The errors quoted for both values of  $F_2(\pi/2)$  include only statistical contributions.

<sup>22</sup> E. D. Cashwell and C. J. Everett, *A Practical Manual on the Monte Carlo Method for Random Walk Problems* (Pergamon Press, Inc., New York, 1959).